Sphalerite−Chalcopyrite Polymorphism in Semimetallic $ZnSnSb_2$

Andreas Tengå,[†] F. Javier García-García,[‡] Arkady S. Mikhaylushkin,[†] Beatriz Espinosa-Arronte,[§] Magnus Andersson,[§] and Ulrich Häussermann*,[†]

Inorganic Chemistry, Stockholm University, SE-10691 Stockholm, Sweden, Max-Planck Institute for Solid State Research, Heisenbergstrasse 1, D-70569 Stuttgart, Germany, and Solid State Physics, IMIT, Royal Institute of Technology, KTH Electrum 229, SE-16440 Kista, Sweden

Received July 21, 2005. Revised Manuscript Received September 5, 2005

We have investigated the system $ZnSnSb_2$ in the course of our attempts to modify thermoelectric Zn−Sb frameworks. $ZnSnSb_2$ is only accessible when employing Sn as reactive flux in the synthesis. The material shows an order−disorder transition in the temperature interval between 225 and 240 °C and decomposes peritectically at about 360 °C. The high-temperature form of $ZnSnSb_2$ adopts the Zn/Sn disordered cubic sphalerite-type structure. Electron microscopy investigations reveal that samples quenched from 350 °C already contain domains of the low-temperature form, which has the Zn/Sn ordered tetragonal chalcopyrite structure. The *c*/*a* ratio of the tetragonal structure is, within experimental errors, identical to the ideal value 2. This gives rise to intricate microtwinning in the low-temperature chalcopyrite form of $ZnSnSb_2$ as obtained in samples quenched from 250 °C. First principles electronic structure calculations demonstrate that the tetragonal low-temperature form of $ZnSnSb_2$ has a narrow band gap of about 0.2 eV. This is in agreement with the semimetallic behavior of the material found from resistivity measurement. The shape of the electronic density of states for $ZnSnSb_2$ is similar to thermoelectric binary Zn−Sb frameworks. However, the thermopower of $ZnSnSb_2$ is rather low with room-temperature values ranging from 10 to 30 μV/K.

1. Introduction

The binary zinc antimonides ZnSb and Zn_4Sb_3 display interesting thermoelectric properties. This holds especially for β-Zn_4Sb_3, which is considered as a state-of-the-art material at moderate temperatures (180−380 °C), closing the gap between low-temperature materials (Bi_2Te_3 based systems) and intermediate temperature materials ($AgSbTe_2$−GeTe-based systems (TAGS)).[1] Peculiar to zinc antimonides are their complex crystal structures, which are combined with narrow gap semiconductor properties.[2−4] In a recent work we could show that Zn−Sb structures actually correspond to weakly polar, s−p bonded frameworks.[5] In this respect zinc antimonides are similar to III−V semiconductors with a simple tetrahedral framework structure; however, they are more electron-poor and thus multicenter-bonded. Interestingly, multicenter bonding appears localized and is confined to rhomboid rings Zn_2Sb_2. Thus, zinc antimonides not only display useful properties but also provide an important contribution toward an understanding of the involved structure-electron count relations typical of the metal−nonmetal border.

We have started to investigate the possibility to modify Zn−Sb frameworks by reacting Zn/Sb mixtures with low-melting metals or semimetals (e.g., In, Sn, Bi, Te). From these experiments we hope to obtain (i) new insights into the intricate chemical bonding mechanism of electron poor s−p bonded intermetallic systems and (ii) a deeper understanding of the origin of thermoelectric properties of the remarkable Zn−Sb materials. In this work we present results from our reactions with Sn. We find that Zn−Sb II−V frameworks may accommodate between 0.8 and 1.5 at. % Sn, depending on the reaction conditions and the kind of framework. These small concentrations can be considered as doping and have interesting consequences to thermoelectric properties.[6] In the case of complex, temperature polymorphic, Zn_4Sb_3 Sn doping also influences decisively structural properties.[6] However, there is only one true ternary phase in the system Zn−Sn−Sb—stoichiometric $ZnSnSb_2$—which can be assessed when reacting mixtures Zn/Sb = 1:2 in excess tin. As a matter of fact, $ZnSnSb_2$ has been known since the late 1960s.[7] The crystal structure of this material was reported as either Zn/Sn disordered cubic sphalerite (ZnS)[8] or ordered tetragonal chalcopyrite.[9] Both structures

* To whom correspondence should be addressed. E-mail: ulrich@inorg.su.se.
† Stockholm University.
‡ Max-Planck Institute for Solid State Research.
§ Royal Institute of Technology.

(1) Caillat, T.; Fleurial, J.-P.; Borshchevsky, A. *J. Chem. Phys. Solids* **1997**, *58*, 1119.
(2) Snyder, G. J.; Christensen, M.; Nishibori, E.; Caillat, T.; Iversen, B. B. *Nat. Mater.* **2004**, *3*, 458.
(3) Cargnoni, F.; Nishibori, E.; Rabiller, P.; Bertini, L.; Snyder, G. J.; Christensen, M.; Gatti, C.; Iversen, B. B. *Chem. Eur. J.* **2004**, *10*, 3861.
(4) Nylén, J.; Andersson, M.; Lidin, S.; Häussermann, U. *J. Am. Chem. Soc.* **2004**, *126*, 16306.
(5) Mikhaylushkin, A. S.; Nylén, J.; Häussermann, U. *Chem. Eur. J.* **2005**, *11*, 4912−4920.
(6) Nylén, J.; Andersson, M.; Lidin, S.; Häussermann U. Unpublished results.
(7) Shay, J. L.; Wernick, J. H. *Ternary Chalcopyrite Semiconductors: Growth, Electronic Properties, and Applications*; Pergamon Press: New York, 1975.
(8) Goryunova, N. A.; Baranov, B. V.; Grigoreva, V. S.; Kradinova, L. V.; Maksimova, V. A.; Prochukhan, V. D. *Izv. Akad. Nauk SSSR, Neorg. Mater.* **1968**, *4*, 1060.

10.1021/cm0516053 CCC: $30.25
Published on Web 10/28/2005

represent simple tetrahedral frameworks, which fits the average electron count of 4 e/atom. Interestingly, bonding in $ZnSnSb_2$ follows the simple octet rule, whereas Zn−Sb frameworks display complex multicentered bonding patterns.[5]

There are several open questions connected with $ZnSnSb_2$. First, its actual crystal structure should be unambiguously determined. At the moment it is not clear whether the material adopts the cubic sphalerite or tetragonal chalcopyrite structure. If the material displays polymorphism, the temperature stability ranges of the different phases should be established. Second, it has been proposed that $ZnSnSb_2$ can be alloyed with Sn to form solid solutions $ZnSnSb_2-Sn_4$.[9] However, explicit homogeneity range and crystal structure of this solid solution have not been reported. Finally, in the light of the interesting thermoelectric performance of Zn−Sb frameworks the characterization of some thermoelectric properties of this material is desirable.

2. Experimental Section

2.1. Synthesis and Characterization. Mixtures of Zn (ABCR, 99.9%) and Sn and Sb (ABCR, 99.999%) with an atomic ratio of 1:2:5 were pressed into pellets and loaded into specially prepared quartz ampules.[10] These ampules contained the reaction mixture at the bottom and a layer of coarsely crushed quartz glass fixed by a plug of quartz wool at the top. Sealed ampules were put into a quartz wool insulated reaction container made of stainless steel, which was subsequently placed into a furnace. The reaction mixture was first heated to 650 °C for 12 h to ensure complete melting of the metals. During this time containers were periodically shaken. Subsequently, the temperature of the homogeneous melt was lowered at rates between 2 and 20 °C/h to a holding temperature between 250 and 350 °C. After the temperature was held for 48 h, the reaction container was turned upside down into a centrifuge, which was operated at 3000 rpm for 3 min. The ampule was opened and the crystalline product was collected from the top of the quartz wool plug. Phase characterization was performed by powder X-ray diffraction patterns taken on a Guinier powder camera with Cu $K\alpha_1$ radiation ($\lambda = 1.540562$ Å) and by compositional analysis with EDX (energy-disperse X-ray) spectroscopy in a JEOL 820 scanning electron microscope. Lattice constants were obtained by least-squares refinements of the indexed powder patterns using the PIRUM program.[11] Specimens for electron microscopy studies were prepared by crushing and dispersing the samples onto holey-carbon coated copper grids. These grids were examined in a Philips CM30 transmission electron microscope operated at 300 kV.

2.2. Electronic Structure Calculations. Calculations of the total energies were performed in the framework of the frozen core all-electron Projected Augmented Wave (PAW) method,[12] which is implemented in the program VASP.[13] The cutoff energy for the plane wave expansion was set to 350 eV. The cutoff for the augmentation charges was set to 550 eV. Exchange and correlation effects were treated with the generalized gradient approximation (GGA).[14] The integration over the Brillouin zone (BZ) was done on a grid of special k-points determined according to the Monkhorst-Pack scheme, using converged k-point grids.[15] The atomic position parameters were relaxed until forces had converged to at least less than 0.005 eV/Å. Equilibrium volume and lattice shape were relaxed as well. The relaxation procedure and accurate total energy calculations were done with the linear tetrahedron method with Blöchl corrections.[16] All necessary convergence tests were performed and total energies were converged to within 0.1 meV/atom.

Zn/Sn site disorder in the cubic disordered phase was modeled within the special quasirandom structures (SQS's), which mimic random atomic distribution for several coordination shells in a supercell.[17] We employed two supercells containing 16 and 32 atoms, respectively. To generate Zn/Sn distributions with required correlation functions according to SQS, we made use of a Metropolis-like algorithm.[18] The N_k correlation functions that we want to match determine a vector σ_j in an N_k-dimensional space. Starting from an arbitrary initial configuration corresponding to some vector σ_j', a particular pair of atoms of different kind, chosen at random, is considered and a vector σ_j'' corresponding to an exchange of the two atoms is calculated. If the distance in the N_k dimensional space between σ_j'' and σ_j is less than the distance between σ_j' and σ_j, the exchange is accepted; otherwise, the initial configuration is kept. The procedure is repeated until a configuration sufficiently close to the one required is generated. For the 32 atom supercell a Zn/Sn distribution was obtained where all short-range order parameters are equal to zero up to the seventh coordination shell. This cell can be considered as a very good approximation for randomly disordered cubic sphalerite. In contrast, the distribution of Zn and Sn atoms in the 16 atom supercell corresponds to a partially ordered one.

2.3. Thermal Property Measurements. The thermal behavior of powdered and single crystalline samples of $ZnSnSb_2$ was investigated by differential thermal analysis (DTA-TG, Setaram Labsys 1600). If visible, traces of Sn on the surface of the material were carefully removed by scratching and polishing. Samples were placed in a steel container and the temperature was raised from 40 °C to either 300 or 400 °C. The experiments were performed under a flow of dry Ar and with temperature increase rates between 5 and 10 °C /min.

2.4. Physical Property Measurements. Resistivity and thermopower measurement were performed on crystalline rods as obtained from flux synthesis. For resistivity measurements a four-point in-line contact arrangement was employed. Contacts were prepared by applying strips of liquid silver paint (Demetron D200), which were dried in air. Resistances were continuously measured as a potential drop of a generated current rendered during cooling and heating in an interval between 100 and 300 K. For thermopower measurements, the sample was attached with silver paint to the hot and cold side of the sample holder, respectively. The thermoelectric voltage U was measured for different temperature gradients ΔT between the two sides. A straight line was fitted to $U(\Delta T)$, which has the slope $dU/d\Delta T = S_w - S_s$ where S_s is the thermopower of the sample and S_w is the thermopower of the connecting wires. When determining S_s, data from a calibration run of the sample holder (using a Pb wire with known thermopower) was used in order to compensate for S_w.

(9) Vaipolin, A. A.; Kradinova, L. V.; Prochukhan, V. D. *Sov. Phys. Crystallogr.* **1971**, *15*, 703.
(10) Boström, M.; Hovmöller, S. *J. Solid State Chem.* **2000**, *153*, 398.
(11) Werner, P-.E. *Ark. Kemi* **1969**, *31*, 513.
(12) (a) Blöchl, P. E. *Phys. Rev. B* **1994**, *50*, 17953. (b) Kresse, G.; Joubert, J. *Phys. Rev. B* **1999**, *59*, 1758.
(13) (a) Kresse, G.; Hafner, J. *J. Phys. Rev.* B **1993**, *48*, 13115. (b) Kresse, G.; Furthmüller, J. *J. Comput. Mater. Sci.* **1996**, *6*, 15.
(14) (a) Wang, Y.; Perdew, J. P. *Phys. Rev. B* **1991**, *44*, 13298. (b) Perdew, J. P.; Chevary, J. A.; Vosko, S. H.; Jackson, K. A.; Pederson, M. R.; Singh, D. J.; Fiolhais, C. *Phys. Rev. B* **1992**, *46*, 6671.
(15) Monkhorst, H. J.; Pack, J. D. *Phys. Rev. B* **1976**, *13*, 5188.
(16) Jepsen, O.; Andersen, O. K. *Solid State Commun.* **1971**, *9*, 1763. Blöchl, P. E.; Jepsen, O.; Andersen, O. K. *Phys. Rev. B* **1994**, *49*, 16223.
(17) Zunger, A.; Wei, S. H.; Ferreira, L. G.; Bernard, J. E. *Phys. Rev. Lett.* **1990**, *65*, 353.
(18) (a) Simak, S. I.; Ruban, A. V.; Abrikosov, I. A.; Skriver, H. L.; Johansson, B. *Phys. Rev. Lett.* **1998**, *81*, 188. (b) Simak, S. I. SQS32 (unpublished).

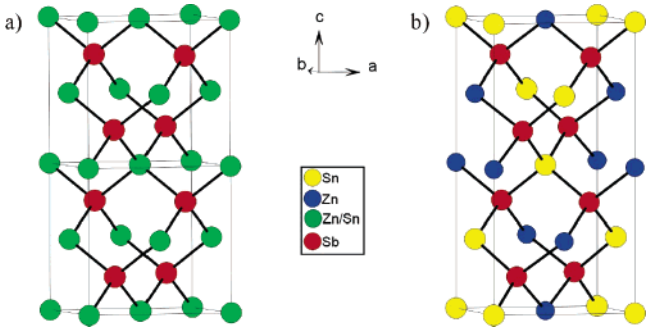

Figure 1. Structures of $ZnSnSb_2$. (a) Zn/Sn disordered cubic sphalerite and (b) Zn/ Sn ordered tetragonal chalcopyrite. Red, blue, and yellow circles denote Sb, Zn, and Sn atoms, respectively. Green circles indicate Zn/Sb random disorder.

3. Results and Discussion

$ZnSnSb_2$ belongs to the class of II−IV−V_2 (ABC_2) materials which all adopt the tetragonal chalcopyrite structure (space group $I\bar{4}2d$, $Z = 4$).[7] In this structure each A- and B-atom are tetrahedrally coordinated by four C-atoms while the C atoms are tetrahedrally coordinated by two A-atoms and two B-atoms in an ordered manner. The atoms occupy the following positions: A in 4a (0,0,0), B in 4b (0,0,$^1/_2$), and C in 8d (x,$^1/_4$,$^1/_8$). A random distribution of A(II) and B(IV) atoms produces the cubic sphalerite (zinc blende) structure. Thus, the chalcopyrite structure can be considered as a superstructure of the sphalerite structure with ideal parameters $c/a = 2$ and $x_C = {}^1/_4$. For II−IV−V_2 systems c/a ratios are typically slightly lower than 2 (around 1.9) and $x_C = 0.22-0.24$. Many of these systems display a high-temperature phase transition to the sphalerite structure (Figure 1).

$ZnSnSb_2$ can only be prepared from reaction mixtures containing a large excess of Sn, i.e., where Sn is employed as reactive flux.[9] We found that ratios Zn:Sb:Sn = 1:2:x with $x > 4$ result in a single-phase product consisting of millimeter-sized, mostly agglomerated, rod or block shaped crystals (Figure 2). In the applied melt-centrifugation synthesis method $ZnSnSb_2$ can be obtained within an annealing temperature window between 240 and 360 °C, which is in agreement with earlier observations.[19] The lower limit is set by the crystallization of excess Sn. Above 360 °C no solid product is formed. This behavior points to a peritectic formation of $ZnSnSb_2$. We performed about 30 synthesis reactions where the Sn content in the reaction mixture, the cooling rates, and the holding temperature has been varied. The obtained products were virtually identical. Only reflections from the cubic sphalerite structure type were observed in the X-ray powder diffraction patterns. The refined lattice parameter varied slightly but significantly between 6.2798(2) and 6.2849(2) Å. There is no obvious correlation between this variation and the applied reaction conditions. Extensive compositional analysis of the products by using EDX spectroscopy never showed any significant deviation from the composition ABC_2 (i.e., 25 at. % Zn, 25 at. % Sn, 50 at. % Sb) and as a result we can rule out the proposed existence of a solid solution $(ZnSnSb_2)_{1-x}Sn_{4-x}$. Importantly, the

(19) Khudolii, V. A.; Golovei, M. I.; Novoselova, A. V. *Dokl. Akad. Nauk SSSR* **1976**, *228*, 1126.

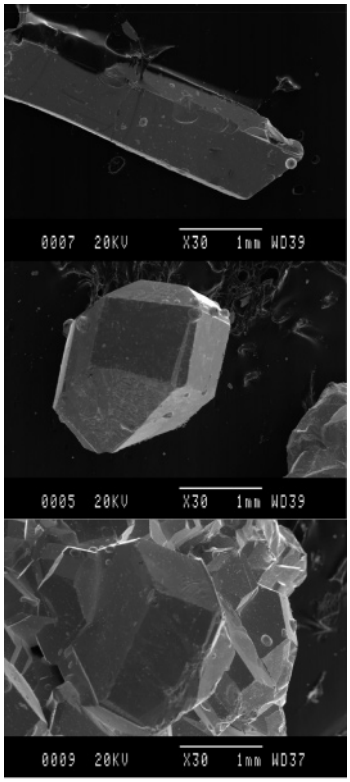

Figure 2. SEM pictures of $ZnSnSb_2$ crystals from a sample annealed at 250 °C.

tetragonal chalocopyrite structure for $ZnSnSb_2$ cannot be detected by using powder diffraction techniques with in-house instrumentation. Therefore, if this structure is adopted, the parameters have to be very close to the ideal values $c/a = 2.0$ and $x_{Sb} = {}^1/_4$ and tetragonal symmetry is primarily the result of Zn/Sn ordering.

The investigation of several crystals on an image plate single-crystal diffractometer revealed the presence of weak superstructure reflections in addition to the set of Bragg reflections from the basic sphalerite structure type. Indexing of all observed reflections could be done by assuming a doubling of the cubic basic unit cell along all symmetry equivalent directions $\langle 100\rangle_p$ (p for parent or basic structure). However, attempts to resolve the superstructure from X-ray data were unsuccessful. Subsequent electron diffraction studies clearly showed that this $2 \times 2 \times 2$ superstructure is fictitious and arises from an intricate domain twinning of the tetragonal chalcopyrite structure type for $ZnSnSb_2$. Additionally, experiments in the electron microscope revealed different degrees of Zn/Sn ordering as a function of annealing temperature.

Figure 3 presents results from the electron diffraction studies. Figures 3a−d show typical electron diffraction patterns, EDPs, recorded in crystals from samples annealed at 350 °C. In Figure 3a a EDP down $\langle 100\rangle_p$ is shown, which reveals well-defined weak satellite reflections of the type $\mathbf{q} = \pm{}^1/_4\,\langle 024\rangle_p^*$. Experiments by moving the incident beam of electrons to diffract in different areas of the same crystal allowed us to conclude (i) that the modulation wave vector changes from area to area and (ii) that only one of the two possible equivalent modulation wave vectors down every $\langle 100\rangle_p$ is excited at any local domain. Such a result is more

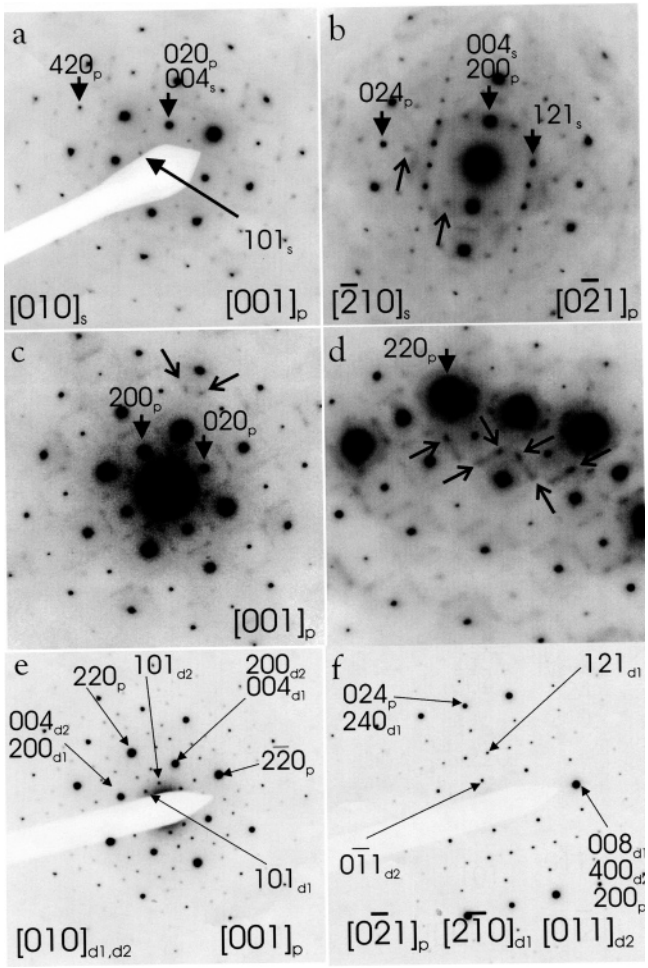

Figure 3. Typical EDPs down $\langle 100\rangle_p$ (a) and $[1\bar{2}0]_p$ (b) from a crystal annealed at 350 °C. The EDP in (c) was recorded in a different crystal down $\langle 100\rangle_p$; a pattern slightly away from the exact Bragg conditions is shown in (d). The presence of well-defined weak satellite reflections of the type $\mathbf{q} = \pm^1/_4\ \langle 024\rangle_p^*$ along with the different intensity in the satellite reflections stemming from different twins domains are clearly visible in (a) and (b). The presence of highly structured diffuse scattering is apparent in (c). Its condensation into reflections is seen in (d). The EDPs presented in (e) and (f) are from a sample annealed at 250 °C. Indexing is presented for the different twin domains present, as well as for the corresponding directions in the sphalerite basic structure.

apparent in the EDP taken down $[0\bar{2}1]_p$ (Figure 3b), where clear differences in the intensity of the satellite reflections from different twins domains are observed. This EDP is indexed according to the strongest present twin domain; the weak satellite reflections from the second domain are indicated by arrowheads. Thus, all observed reflections from any single domain can be indexed by using an expression of the type $\mathbf{H} = \mathbf{G} \pm {}^1/_4\ [024]_p^*$, where **G** are Bragg reflections from the basic cubic (sphalerite) structure. The resulting new reciprocal lattice vectors are $\mathbf{a_s}^* = \mathbf{a_p}^*$, $\mathbf{b_s}^* = \mathbf{b_p}^*$, $\mathbf{c_s}^* = {}^1/_2\mathbf{c_p}^*$ (s for superstructure) and the corresponding real space unit cell vectors are given by $\mathbf{a_s} = \mathbf{a_p}$, $\mathbf{b_s} = \mathbf{b_p}$, $\mathbf{c_s} = \mathbf{2c_p}$. The observed extinction conditions fully agree with space group *I-42d* which strongly indicates that the superstructure corresponds to the tetragonal chalcopyrite structure where *c*/*a* takes the ideal value 2.

The EDP presented in Figure 3c was recorded in a different crystal and discloses pronounced and highly structured diffuse scattering. Additionally, weak satellite reflections of the type $\mathbf{q} = \pm^1/_4\ \langle 024\rangle_p^*$ are visible, but they are much more blurred and diffuse compared to those in Figure 3a. As a matter of fact, they form part of the lines of diffuse scattering running exactly perpendicular to $\langle 100\rangle_p^*$. This becomes more apparent after tilting off the crystal a few degrees away from the exact Bragg condition (Figure 3d). The occurrence of diffuse scattering should be due to the presence of Zn/Sn compositional short-range ordering in the cubic basic structure, which embeds domains of completely ordered tetragonal superstructure. The observed reciprocal space distribution of the diffuse diffracted intensity reproduces the expected shape of purely compositional short-range ordering in a sphalerite type structure, as reported in ref 20.

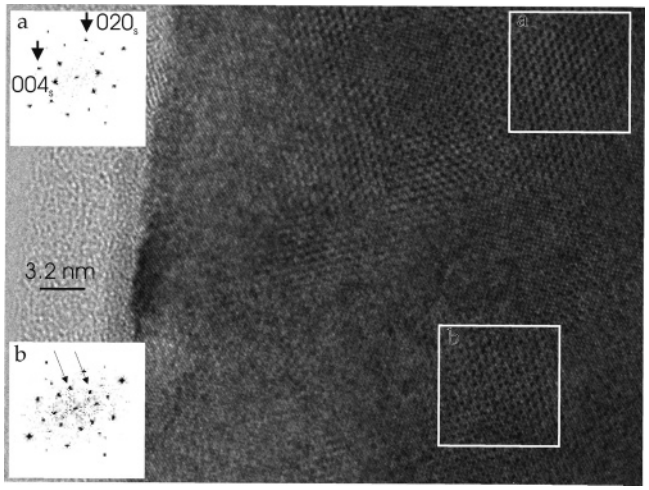

Figure 4. High-resolution image of a crystal oriented down $[010]_{s,p}$ from a sample annealed at 250 °C. The insets are the digital diffraction patterns obtained in the squared areas.

Figures 3e and 3f present two EDPs from a sample annealed at 250 °C. The patterns are indexed according to the basic structure and to the different observed superstructure twinned domains (subscripts d1 and d2). Tilting experiments carried out in the same way as for 350 °C samples showed the complete absence of diffuse scattering associated with compositional short-range ordering.[21] This strongly indicates that the ordered tetragonal chalcopyrite structure has fully developed at lower temperatures. Careful analysis of the reciprocal lattice showed that all possible twin domains are present in all crystals. Figure 4 shows a high-resolution image of a crystal annealed at 250 °C oriented down $[010]_{s,p}$. The domains, as seen in the image, have typically a size of less than 10 nm. Analysis of the recorded images reveals a complicated situation when interpreting the observed contrast. In the insets we present the digital diffraction patterns corresponding to the squared areas. While in (a) one single domain is present, a second domain appears in (b). This is evident from the presence of the satellite reflections indicated by arrowheads. As a matter of fact, the majority of supposedly single domains in 250 °C $ZnSnSb_2$ give rise to digital diffraction patterns similar to that of (b). This means that

(20) Sauvage, M.; Parthé, E. *Acta Crystallogr. A*, **1974**, *30*, 239.
(21) At this point we should mention that we also observed diffuse scattering in 250 °C annealed crystals. This scattering (i.e., sheets of diffuse intensity in {110}*) is conspicuously different from that observed in high-temperature annealed crystals and characteristic for displacive short-range order [see e.g. Withers, R. L.; Welberry, T. R.; Pring, A.; Tenailleau, C.; Liu, Y. *J. Solid State Chem.* **2004**, *178*, 655].

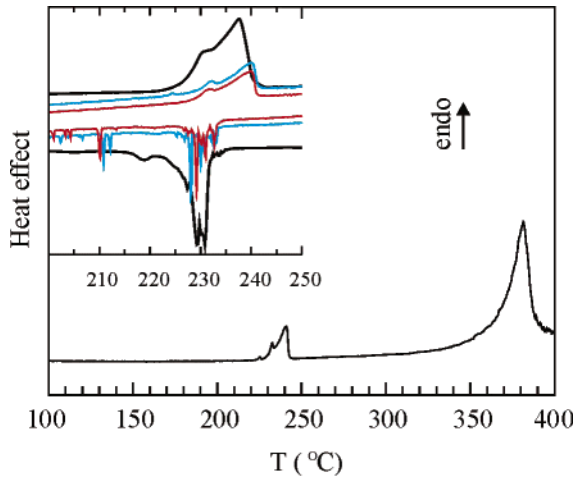

Figure 5. DTA curves for $ZnSnSb_2$ obtained from a 250 °C annealing synthesis reaction. The inset shows the heat effect of the order−disorder transition between 200 and 250 °C for a sample consisting of several crystals (cycled two times, red and blue lines, respectively) and a finely ground sample (black lines).

they are actually composed by two, or more, twin domains sitting on top of each other.

In conclusion, we find that $ZnSnSb_2$ indeed adopts the tetragonal chalcopyrite structure. Electron diffraction experiments show that this phase forms continuously from the disordered cubic sphalerite type: Annealing at 350 °C produces $ZnSnSb_2$ where Zn and Sn atoms are short range ordered along with domains of fully ordered tetragonal structure. When samples are annealed at a lower temperature, 250 °C, the tetragonal chalcopyrite structure develops completely but in a complicated, domain twinned, form. The slightly varying cubic cell parameter of our samples is probably due to the fact that they are composed of different ratios of short-range ordered sphalerite and chalcopyrite modification. In chalcopyrite $ZnSnSb_2$ all possible twin domains are present at roughly the same proportion. The observed fine scale twinning is most likely a consequence of the peculiar c/a ratio of the tetragonal structure, which is virtually identical to the ideal value of 2. This in turn gives a perfect coherence between different domains in high-resolution experiments. Interestingly, the same situation has been reported for $ZnSnAs_2$ and $ZnSnP_2$.[22−25] Also for these compounds the chalcopyrite c/a ratio is very close to 2; however, the tetragonal structure appears more pronounced and as larger domains, which allowed the study of its twinning by single-crystal X-ray diffraction. For $ZnSnAs_2$ it is even possible to quench the disordered sphalerite structure.[23]

Figure 5 shows various DTA traces for $ZnSnSb_2$ obtained from a 250 °C annealing reaction. The thermal behavior of differently annealed samples is basically identical. We observe an endothermic effect in the temperature range 225−240 °C, which is reversible. This effect is attributed to the chalcopyrite−sphalerite order−disorder transition. The onset of the decomposition of $ZnSnSb_2$ takes place at around 360 °C. The X-ray powder diffraction pattern of a DTA 400 °C heated and cooled sample showed a complex mixture of ZnSb, SnSb, traces of β-Sn, and partly reformed $ZnSnSb_2$. We mention that the related systems $ZnSnAs_2$ and $ZnSnP_2$ have considerably higher melting temperatures (740 and 930 °C, respectively).[7] The appearance of the heat effect connected with the order−disorder transition indicates that this process is actually composed of several steps. This is understandable against the background that the transition is accompanied by the formation of a complicated, twinned microstructure. Otherwise, from group theoretical considerations the sphalerite−chalcopyrite ordering process can take place in a continuous, second-order fashion.[26] The peritectic melting temperature of $ZnSnSb_2$ is in agreement with our observation from synthesis which does not afford a solid product above 360 °C. Although the order−disorder transition takes place before 250 °C, it does not seem to be possible to quench pure $ZnSnSb_2$ sphalerite.

We performed first-principles density functional calculations in order to analyze the electronic structure of $ZnSnSb_2$. The results of the computational structure optimization for tetragonal $ZnSnSb_2$ was $c/a = 2.01$ and $x_{Sb} = 0.2237$ which agrees with the experimental finding of the chalcopyrite structure having structural parameters close to ideal values. However, the parameter x_{Sb} deviates considerably from the ideal value 0.25, which implies that in tetrahedra $SbZn_2Sn_2$ Sb atoms are displaced from the center toward the edges occupied by Zn atoms. In the computationally relaxed structure distances Sb−Zn and Sb−Sn are 2.67 and 2.87 Å, respectively. The density of states for tetragonal $ZnSnSb_2$ at equilibrium volume displays a narrow band gap of 0.2 eV at the Fermi level (Figure 6a). The shape of the valence band is very similar to the one we found for thermoelectric Zn−Sb framework structures.[5] The narrow band gap of the tetragonal structure is rapidly closed when Zn/Sn disorder is introduced. This is shown in Figures 6b and 6c where the DOS for two model structures with different distributions of Zn and Sn atoms—simulating different degrees of Zn/Sn disorder—are displayed. In the 16 atom supercell Zn and Sn atoms are partially ordered, whereas the 32 atom supercell should correspond closely to randomly disordered cubic $ZnSnSb_2$ with the sphalerite structure. The total energy is lowest for the completely ordered tetragonal structure; the 16 and 32 atom structures are 14 and 44 meV/atom higher in energy.

Finally, we turn to the characterization of some properties of $ZnSnSb_2$ relevant to thermoelectricity. Resistivity measurements are shown in Figure 7a. The room-temperature value of the specific resistivity ρ of $ZnSnSb_2$ is around 0.3 mΩcm. Between 80 and 300 K ρ varies only little with temperature. This semimetallic behavior is in agreement with the calculated electronic structure. The presented three measurements illustrate that the material $ZnSnSb_2$ is not homogeneous; even crystals from the same sample may produce significantly different results. This is not surprising considering the complicated microstructure of $ZnSnSb_2$.

(22) Pfister, H. *Acta Crystallogr.* **1963**, *16*, 53.
(23) Vaipolin, A. A.; Kesamanly, F. P.; Rud, Y. V. *Izv. Akad. Nauk SSSR, Neorg. Mater.* **1967**, *3*, 974.
(24) Vaipolin, A. A.; Goryunova, N. A.; Kleshchinskii, L. I.; Loshakova, G. V.; Osmanov, E. O. *Phys. Status Solidi* **1968**, *29*, 435.
(25) Seryogin, G. A.; Nikishin, S. A.; Temkin, H.; Mintairov, A. M.; Merz, J. L.; Holtz, M. *Appl. Phys. Lett.* **1999**, *74*, 2128.
(26) Folmer, J. C. W.; Franzen, H. F. *Phys. Rev. B* **1984**, *29*, 6261.

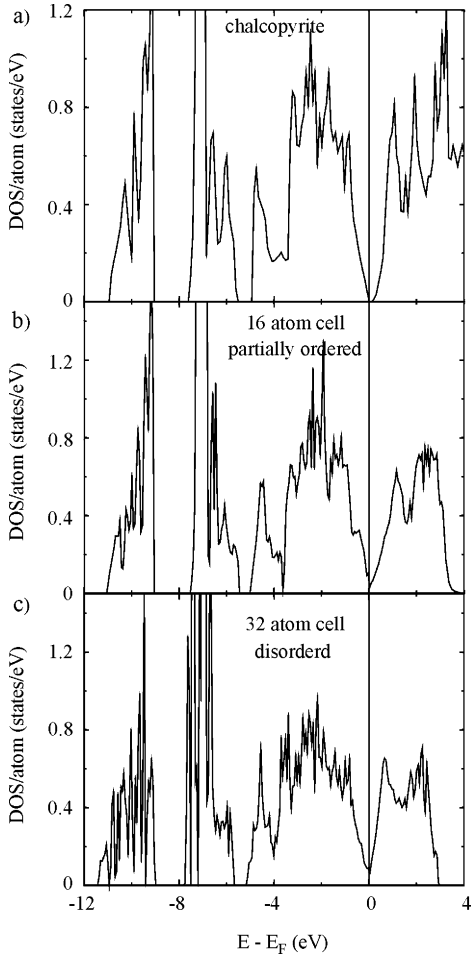

Figure 6. Density of states (DOS) for $ZnSnSb_2$ with the Zn/Sb ordered, tetragonal, chalcopyrite structure (a), with partially Zn/Sn ordering in a 16 atom/unit cell structure (b), and with a random Zn/Sn distribution in a 32 atom unit cell approximating the cubic sphalerite structure (c).

Different degrees of Zn/Sn order as well as size and arrangement of microtwinned domains of the tetragonal form should influence strongly transport properties. This is especially seen in the thermopower measurements (Figure 7b) where room-temperature values vary between about 10 and 30 μV/K. The positive value of S implies that holes are charge carriers in $ZnSnSb_2$. According to its resistivity and thermopower values, $ZnSnSb_2$ represents a rather poor thermoelectric material, although its complex microstructure probably gives rise to a desirable low thermal conductivity κ, which together with S and ρ defines the thermoelectric figure of merit $Z = S^2/\rho\kappa$. Interestingly, it has been stated that compounds with tetrahedral structures typically do not represent good thermoelectric materials.[27] The reason for this is not clear but $ZnSnSb_2$ seems to confirm this observation.

4. Summary

We reinvestigated the system $ZnSnSb_2$ in the course of our attempts to modify thermoelectric Zn−Sb frameworks.

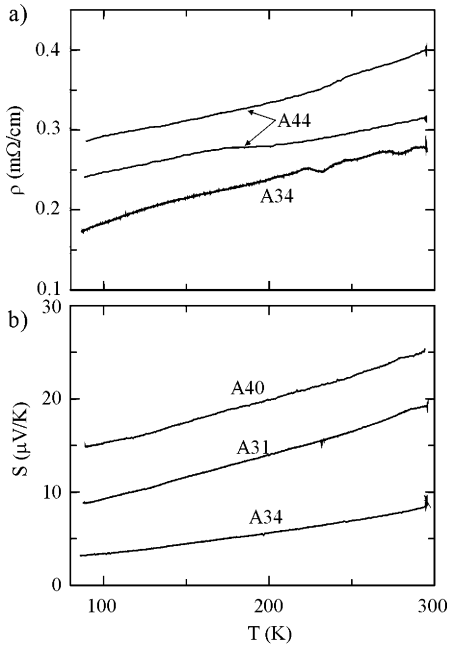

Figure 7. Resistivity ρ (a) and thermopower S (b) of crystalline blocks of $ZnSnSb_2$ obtained from different synthesis reactions. (A44: annealing temperature 250 °C/annealing time: 2 d/cooling rate from 650 °C: 2 K/h; A34: 300 °C/2 d/20 K/h; A40: 250 °C/24 h/20 K/h; A31: 250 °C/11 d/20 K/h).

$ZnSnSb_2$ is only accessible when employing Sn as reactive flux in the synthesis. The material shows an order−disorder transition in the temperature interval between 225 and 240 °C and decomposes peritectically at about 360 °C. The high-temperature form of $ZnSnSb_2$ adopts a disordered cubic sphalerite structure where Zn and Sn atoms are randomly distributed over the same crystallographic position. This phase, however, cannot be obtained in a pure form from synthesis. Electron microscopy investigations reveal that samples quenched from 350 °C already contain domains of the low-temperature form, which has the Zn/Sn ordered tetragonal chalcopyrite structure. Additionally, pronounced and highly structured diffuse scattering indicate a substantial degree of Zn/Sb ordering present in high-temperature samples. Interestingly, the c/a ratio of the tetragonal structure is virtually identical to the ideal value 2. This gives rise to intricate microtwinning in the low-temperature chalcopyrite form of $ZnSnSb_2$ as obtained in samples quenched from 250 °C. According to first-principles electronic structure calculations, the tetragonal low-temperature form of $ZnSnSb_2$ has a narrow band gap of about 0.2 eV. This is in agreement with the semimetal behavior of the material in resistivity measurements. Although the electronic structure of $ZnSnSb_2$ is qualitatively similar to thermoelectric binary Zn−Sb frameworks, its thermopower is rather low as room-temperature values range from 10 to 30 μV/K.

Acknowledgment. This work was supported by the Swedish Research Council (VR).

CM0516053

(27) Mahan, G. D. In *Solid State Physics Vol. 51*; Ehrenreich, H., Spaepen, F., Eds.; Academic Press: New York, 1997; p 81.